Spectrum of Excess Partial Molar Absorptivity. I. Near Infrared Spectroscopic Study of Aqueous Acetonitrile and Acetone

ARTICLE *in* THE JOURNAL OF PHYSICAL CHEMISTRY B · SEPTEMBER 2009

Impact Factor: 3.3 · DOI: 10.1021/jp901934c · Source: PubMed

Spectrum of Excess Partial Molar Absorptivity. I. Near Infrared Spectroscopic Study of Aqueous Acetonitrile and Acetone

Yoshikata Koga,*[,†,‡] Fumie Sebe,[‡,§] Takamasa Minami,[‡,∥] Keiko Otake,[‡,⊥] Ken-ichi Saitow,[#,∇,○,◆] and Keiko Nishikawa[‡]

Department of Chemistry, The University of British Columbia, Vancouver, BC Canada, V6T 1Z1, Graduate School of Advanced Integration Sciences, Chiba University, Chiba 263-8522, Japan, Power & Industrial Systems Research & Development Center, Power Systems Company, Toshiba, Yokohama 235-8523, Japan, Material & Process Development Center, TDK, Narita 286-8588, Japan, R&D Mazda, Yokohama 221-0022, Japan, Department of Physics, Chiba University, Chiba 263-8522, Japan, Natural Science Center for Basic Research and Development, Hiroshima University, Higashi Hiroshima 739-8526, Japan, Graduate School of Science, Hiroshima University, Higashi Hiroshima 739-8526, Japan, and PRESTO, Japan Science and Technology Agency, Kawaguchi 332-0012, Japan

Received: March 2, 2009; Revised Manuscript Received: June 8, 2009

We study the mixing schemes or the molecular processes occurring in aqueous acetonitrile (ACN) and acetone (ACT) by near-infrared spectroscopy (NIR). Both solutions (any other aqueous solutions) are not free from strong and complex intermolecular interactions. To tackle such a many-body problem, we first use the concept of the excess molar absorptivity, ε^E, which is a function of solute mole fraction in addition to that of wavenumber, ν. The plots of ε^E calculated from NIR spectra for both aqueous solutions against ν showed two clearly separated bands at 5020 and 5230 cm^{-1}; the former showed negative and the latter positive peaks. At zero and unity mole fractions of solute, ε^E is identically zero independent of ν. Similar to the thermodynamic excess functions, both negative and positive bands grow in size from zero to the minimum (or the maximum) and back to zero, as the mole fraction varies from 0 to 1. Since the negative band's ν-locus coincides with the NIR spectrum of ice, and the positive with that of liquid H_2O, we suggest that on addition of solute the "ice-likeness" decreases and the "liquid-likeness" increases, reminiscent of the two-mixture model for liquid H_2O. The modes of these variations, however, are qualitatively different between ACN−H_2O and ACT−H_2O. The former ACN is known to act as a hydrophobe and ACT as a hydrophile from our previous thermodynamic studies. To see the difference more clearly, we introduced and calculated the excess partial molar absorptivity of ACN and ACT, ε_N^E and ε_T^E, respectively. The mole fraction dependences of ε_N^E and ε_T^E show qualitatively different behavior and are consistent with the detailed mixing schemes elucidated by our earlier differential thermodynamic studies. Furthermore, we found in the H_2O-rich region that the effect of hydrophobic ACN is acted on the negative band at 5020 cm^{-1}, while that of hydrophilic ACT is on the positive high-energy band. Thus, the present method of analysis adds more detailed insight into the difference between a hydrophobe and a hydrophile in their effects on H_2O.

Introduction

Aqueous solutions, any mixtures for that matter, are governed by the so-called "many-body problem". There are strong and complex interactions among constituents that dictate the holistic nature of the assembly. It is often far from that which is imaginable from the sum of the properties of individual constituents. In solution thermodynamics, an approach has been used for decades such that the effects of interactions are lumped together into the excess thermodynamics function.[1] For the mixture consisting of n_B moles of B and n_W moles of W, for example, the total enthalpy of the system, H, is written as

$$H = n_B H_B^0 + n_W H_W^0 + H^E = n_B H_B^0 + n_W H_W^0 + N H_m^E \quad (1)$$

where H_B^0 and H_W^0 are the molar enthalpies of pure B and W, respectively, and $N = n_B + n_W$. H^E is the excess enthalpy of the system that contains all the effects due to the many-body problem. In the second equality in eq 1, the relation $H_m^E = H^E/N$ was used. The philosophical background of eq 1 is that (a) the existence of the many-body problem is explicitly recognized and (b) all such effects are lumped together into one term H^E. It is therefore up to us to dig out the detailed information about the interactions among constituents of H^E. We have made an attempt at such an endeavor.[2−4] Namely, we determine experimentally the excess partial molar enthalpy of B or W, H_B^E or H_W^E, by perturbing the system with an infinitesimal increase in n_B (or n_W), the amount of the chosen target component. We then measure the response of the system in terms of H^E. Thus

* Corresponding author. E-mail: koga@chem.ubc.ca.
† The University of British Columbia.
‡ Graduate School of Advanced Integration Sciences, Chiba University.
§ Power Systems Company, Toshiba.
∥ Material & Process Development Center, TDK.
⊥ R&D Mazda.
Department of Physics, Chiba University.
∇ Natural Science Center for Basic Research and Development, Hiroshima University.
○ Graduate School of Science, Hiroshima University.
◆ Japan Science and Technology Agency.

10.1021/jp901934c CCC: $40.75
Published on Web 08/13/2009

$$H_B^E = \left(\frac{\partial H^E}{\partial n_B}\right)_{n_w,p,T} \quad (2)$$

This quantity provides information about B's contribution toward H^E, or the actual enthalpic situation of B in the strongly interacting mixture. We then perturb the system once again by an infinitesimal increase in n_B and see how H_B^E responds to it. We do this by graphical differentiation without resorting to any fitting function. Thus

$$H_{B-B}^E = N\left(\frac{\partial H_B^E}{\partial n_B}\right) = N\left(\frac{\partial^2 H^E}{(\partial n_B)^2}\right) \quad (3)$$

This quantity signifies the effect of incoming B on the actual enthalpic situation of B in the mixture. Hence we call H_{B-B}^E the B−B interaction in terms of enthalpy. The technical details of obtaining H_B^E, H_{B-B}^E, and their entropy and volume analogues are described elsewhere.[3−5] We stress here that both H_B^E and H_{B-B}^E and analogous expressions for other thermodynamic quantities are experimentally accessible and completely model-free. Furthermore, the information contained in H_{B-B}^E is more detailed than that in H_B^E, which in turn is more so than that in H^E. This is our differential approach of digging out the detailed information of H^E.

These higher-order derivative quantities and their temperature and mole fraction dependences have revealed the molecular processes in aqueous solutions, which we call mixing scheme, to an unprecedented depth.[2−4] In particular, we found that acetonitrile (abbreviated as ACN) acts in the same way as other hydrophobic solutes in aqueous solutions.[6,7] Namely, it enhances the hydrogen bond network of H_2O in its immediate vicinity (similar to the classical picture of iceberg formation), but more importantly it reduces progressively the hydrogen bond probability of bulk H_2O away from the solute, as the mole fraction of ACN, x_N, increases. However, the hydrogen bond probability of bulk H_2O remains high enough that the hydrogen bond network is bond-percolated. At $x_N = 0.0094$ at 25 °C (0.0080 at 37 °C), the hydrogen bond probability is reduced to the bond percolation threshold of ice Ih type connectivity, and bulk H_2O loses its characteristic integrity. The mixing scheme up to this mole fraction described above is called Mixing Scheme I. The process of losing the hydrogen bond network connectivity continues to about $x_N = 0.07$ at 25 °C (0.060 at 37 °C), and beyond this point what we call Mixing Scheme II is operative, whereby the solution consists of two kinds of clusters: one rich in H_2O and the other in ACN. When x_N becomes larger than 0.45 at 37 °C, ACN molecules form clusters by themselves in a manner similar to that in the pure state, and H_2O interacts with such clusters almost as a single molecule and hence H_2O loses its characteristics of liquid H_2O. We call this Mixing Scheme III. The two kinds of clusters in Mixing Scheme II mentioned above are reminiscent of Mixing Schemes I and III.

Acetone (ACT), on the other hand, behaves in aqueous solutions as a hydrophile.[6,8] A hydrophile forms hydrogen bonds directly to the existing network of H_2O. Thus, the hydrogen bond network connectivity remains intact. However, the degree of large fluctuations characteristic to liquid H_2O is reduced progressively by breaking H donor/acceptor symmetry enjoyed in pure H_2O. At the mole fraction of ACT, $x_T = 0.08$ at 25 °C, strain within the hydrogen bond network due to the presence of impurity centers (ACT) becomes too much to retain the hydrogen bond connectivity, and the network starts to break down. The process completes its course at about $x_T = 0.24$, and Mixing Scheme II sets in. In the region $x_T > 0.5$ at 25 °C, Mixing Scheme III is operative. The findings by Raman spectroscopy aided by MD calculations[9] are not inconsistent with our conclusions. This Raman study makes use of H_m^E data of ACT−H_2O.[10,11] As described above, H_m^E is a lower derivative than H_B^E (eq 2 with B = ACT) and H_{B-B}^E (eq 3). In view of the power in higher-order derivative thermodynamic quantities in revealing more detailed information discussed above, it was unfortunate the authors did not have a chance to see our paper on ACT−H_2O.[8] We stress that the detail of Mixing I is somewhat different between those for ACN and ACT, but the integrity of H_2O, the bond percolated hydrogen bond network, is equally intact. Mixing Schemes II and III are the same for both hydrophiles and hydrophobes.

Here we use below a similar approach taking explicitly into consideration the many-body problem in the near-infrared (NIR) spectroscopic study on the same aqueous solutions. NIR spectroscopy is powerful, particularly in the range 4600−5500 cm^{-1} where the ν_2 (OH bending) + ν_3 (asymmetric OH stretching) combination band is observed, revealing the effect of temperature rise[12,13] and that of an additional salt[14] on the hydrogen bond nature of H_2O.

Many-Body Problem in Spectroscopy

Beer−Lambert's law states that absorbance, A, is written as

$$A/l = \varepsilon C = \varepsilon(N/V) \quad (4)$$

where ε is the molar absorptivity, l the optical path length, and C the molar concentration. The second equality of eq 4 is written by writing $C = N/V$ where V is the volume through which the light is passing and N is the molar amount of the sample in V. Generally, it is understood that ε is only a function of the wavenumber, ν, of the light passing through the sample and is independent of C. We point out here that if the density becomes high A may no longer be linear to C due to intermolecular interactions, and hence ε becomes a function of C as well as ν. The recognition of this fact is the first step for dealing with the many-body problem in spectroscopic analysis. For a mixture containing n_B moles of B and n_W moles of W, we rewrite it as, following the lead by Li et al.[15] and the far right of eq 1

$$A/l = n_B\varepsilon_B^0(1/V) + n_W\varepsilon_W^0(1/V) + N\varepsilon^E(1/V) \quad (5)$$

where ε_B^0 and ε_W^0 are the molar absorptivity for pure B and W, respectively. For the present mixtures, the molar volume data, V_m, are available for both ACN−H_2O[16] and ACT−H_2O.[17] While the experimentally determined molar volume (or the density) data may not be required for the nonaqueous binary systems studied by Li et al.,[15] they must be used here for the present aqueous solutions that are highly nonideal. We note in passing that the introduction of the concept of ε^E by Li et al.[15] leads them to rank clearly the degree of nonideality of some nonaqueous binary systems, just as H_m^E data would.

Since $V = NV_m$, eq 5 is rewritten as

$$(A/l)V_m = x_B\varepsilon_B^0 + x_W\varepsilon_W^0 + \varepsilon^E \quad (6)$$

x_B and x_W are the mole fraction of B and W. ε_B^0 and ε_W^0 can be separately determined using the values of (A/l) and those of V_m for pure B and W. Thus, the excess molar absorptivity, ε^E, is

calculated by eq 6. We stress here that ε^E is a function of ν as well as x_B (and x_W). As for H^E or H_m^E in eq 1, ε^E contains all the information about the many-body problem of the system. To investigate the ingredient of ε^E in more detail, we follow our thermodynamic study and take the derivative with respect to n_B as in eq 2. Thus

$$\varepsilon_B^E = N\left(\frac{\partial \varepsilon^E}{\partial n_B}\right) = (1 - x_B)\left(\frac{\partial \varepsilon^E}{\partial x_B}\right) \quad (7)$$

This is where we divert from the work by Li et al.[15] in which the obtained ε^E data were subjected to analysis commonly used in spectroscopic studies. Instead of analyzing data on the basis of a model, we learn directly from the behaviors of these model-free ε_B^E data (B = ACT or ACN), as for our differential thermodynamics studies. The second equality on the right is obtained by converting the variable system (n_B, n_W) for the first equality to a more convenient one (x_B, N). According to eq 7, ε_B^E is the effect of perturbing by n_B on the excess molar absorptivity or the excess part of the transition probability of the vibration in question. The latter is related to $|<G|\mu|E>|^2$ at a given $\nu = (E_E - E_G)/h$, where G and E stand for the vibrational wave functions at the ground and the excited states, respectively, and μ is the transition dipole moment. Hence, in theory, ε_B^E provides information about the effect of B on the wave functions of E and/or G at given x_B and ν.

Here we analyze the near-infrared spectra (NIR) of ACN−H_2O and ACT−H_2O according to eqs 6 and 7 and seek any additional information from the present many-body analysis without resorting to any model system, above what we learned from thermodynamic studies using eqs 2 and 3.

Experimental Section

Acetonitrile and acetone (both Analytical Reagent grade, Wako Pure Chemicals Ind.) were used as supplied. H_2O was first deionized and then distilled by Yamato Kagaku Autostill WG201 immediately before use. The aqueous solutions were prepared gravimetrically for ACN. For ACT−H_2O, they were mixed volumetrically using a pipet and a syringe. The mole fraction on ACN, x_N, was directly calculated with at least four significant figures, while for that of ACT, x_T was calculated using the literature density data[18] within three significant figures.

An NIR spectrophotometer was home-constructed. The detail was described fully elsewhere.[14] Absorbance, $A = \log[(I_0 - I_d)/(I - I_d)] = \log[(t - t_d)/(t_0 - t_d)]$, was measured in the range from 4600 to 5500 cm^{-1} targeting the $\nu_2 + \nu_3$ band at about 3 or 6 cm^{-1} intervals. I is the intensity of light and t the transmittance, where subscript 0 stands for the incident, d for the dark background, and none for the sample mixture. It is inevitable that at a large value of A, i.e., peak regions, the uncertainty becomes large since the value of t tends to be small with fewer significant figures. Thus we used a short path length $l = 0.5$ mm to increase the value of t. For ACN−H_2O, a 0.25 mm sample cell was used.

Results and Discussion

Figure 1 shows the results plotted against ν. The raw data are given in the Supporting Information (Table Supp1 for ACN−H_2O and Table Supp2 for ACT−H_2O). Since the spectrometer is of a single beam arrangement,[14] the measurements for t_0, t, and t_d were not made concurrently. Hence there is some danger of introducing a systematic error resulting in an upward or downward shift of the baseline. Several spectra that seem to suffer such effects were removed. Figures 1(a) and (b) are for ACN−H_2O, and Figure 1(c) is for ACT−H_2O. The original nonsymmetric $\nu_2 + \nu_3$ band of pure H_2O skews to the right, to higher wavenumbers, as the mole fraction of ACN or ATC increases. A similar trend has been observed earlier as $NaClO_4$ was added[14] or the temperature was raised.[12,13] This behavior has been interpreted[12−14] that this nonsymmetric band and its mode of changes are due to the existence of three actual distinctive species of H_2O differing in the number of hydrogen bonds of a central H_2O molecule. Thus, the skewing behavior of the band was attributed to the changes in population of each species. Implicit in this treatment is the assumptions that there exist three distinct species differing in the number of hydrogen bonds of a central H_2O molecule and that the absorbance (or its integral) of each species is proportional to their compositions. The reality of the first assumption is still to be debated fully.[13] Regarding the second, our basic stance of the present work is to make an attempt at dealing with the many-body problem head on and hence to recognize a possibility of nonlinearity, even if such three species indeed existed. We thus calculated ε^E from the raw A/l data by eq 6 and plotted in Figures 2(a) and (b) for ACN−H_2O and in Figure 2(c) for ACT−H_2O. We note that the maximum values of ε^E for ACN−H_2O and ACT−H_2O are about 30 mm^{-1} cm^3 mol^{-1} (0.3 cm^{-1} dm^3 mol^{-1} in the usual units) at about 5200 cm^{-1}, and the minimum value is −10 mm^{-1} cm^3 mol^{-1}. These values are quite sizable in comparison with the maximum in $\varepsilon_W^0 \sim 110$ mm^{-1} cm^3 mol^{-1} at about 5150 cm^{-1}: some 30% and 10%. This already hints that the many-body effect is not insignificant.

It is evident in Figure 2 that there are two bands in ε^E: a negative one at about 5000 cm^{-1} and the other positive at about 5200 cm^{-1}. Namely, as x_N or x_T increases, ε^E for the negative 5000 cm^{-1} bands decreases from 0 at pure H_2O to the minimum and increases back to 0 at pure ACN or ACT. That for the positive 5200 cm^{-1} band increases to the maximum and decreases back to 0. We recall that the $\nu_2 + \nu_3$ band for ice peaks at about 5000 cm^{-1} and that for liquid H_2O at about 5200^{-1}.[12,13] Thus, the behavior of ε^E in Figure 2 suggests that on addition of ACN and ACT the "ice-likeness" decreases and the "liquid-likeness" increases. This could be one of the manifestations of the so-called "mixture model" for understanding liquid H_2O.[19,20] This model of course is only a facet of the holistic object, H_2O. A behavior of the $\nu_2 + \nu_3$ band similar to that in Figure 2 was also observed in the difference spectra due to temperature increase.[12,13] In particular, Czarnik-Matusewicz and Pilorz showed that the difference spectra $\Delta A = A_t - A_{20}$ at temperature t from that at 20 °C decreases at about 5000 cm^{-1} and increases at about 5200 cm^{-1}. In addition, they showed that the minimum locus, ν_{min}, monotonously shifts from 5000 to 5040 cm^{-1}, while ν_{max} shifts from 5247 to 5255 cm^{-1} as temperature changes from 25 to 80 °C. Their spectra are "clean" and reveal a subtle variation in the loci of the minimum and the maximum. However, the observed raw data had been subjected to the "pre-processing" including denoising by wavelet transformation,[21,22] baseline correction, and elimination of baseline fluctuation. The details of the latter two treatments are not described. The resulting spectra look very clean. However, how close they are to the reality is to be debated in view of the fact that the spectrometer they used (Nicolet Magna 860) is of a single beam configuration. We present here the raw data as they are, except for removal of obvious poor baseline cases as mentioned above. Figure 2 indicates that while the values of ε^E around the minimum and maximum vary systematically as described above, the ν-loci of the minimum and the maximum shift about ±20

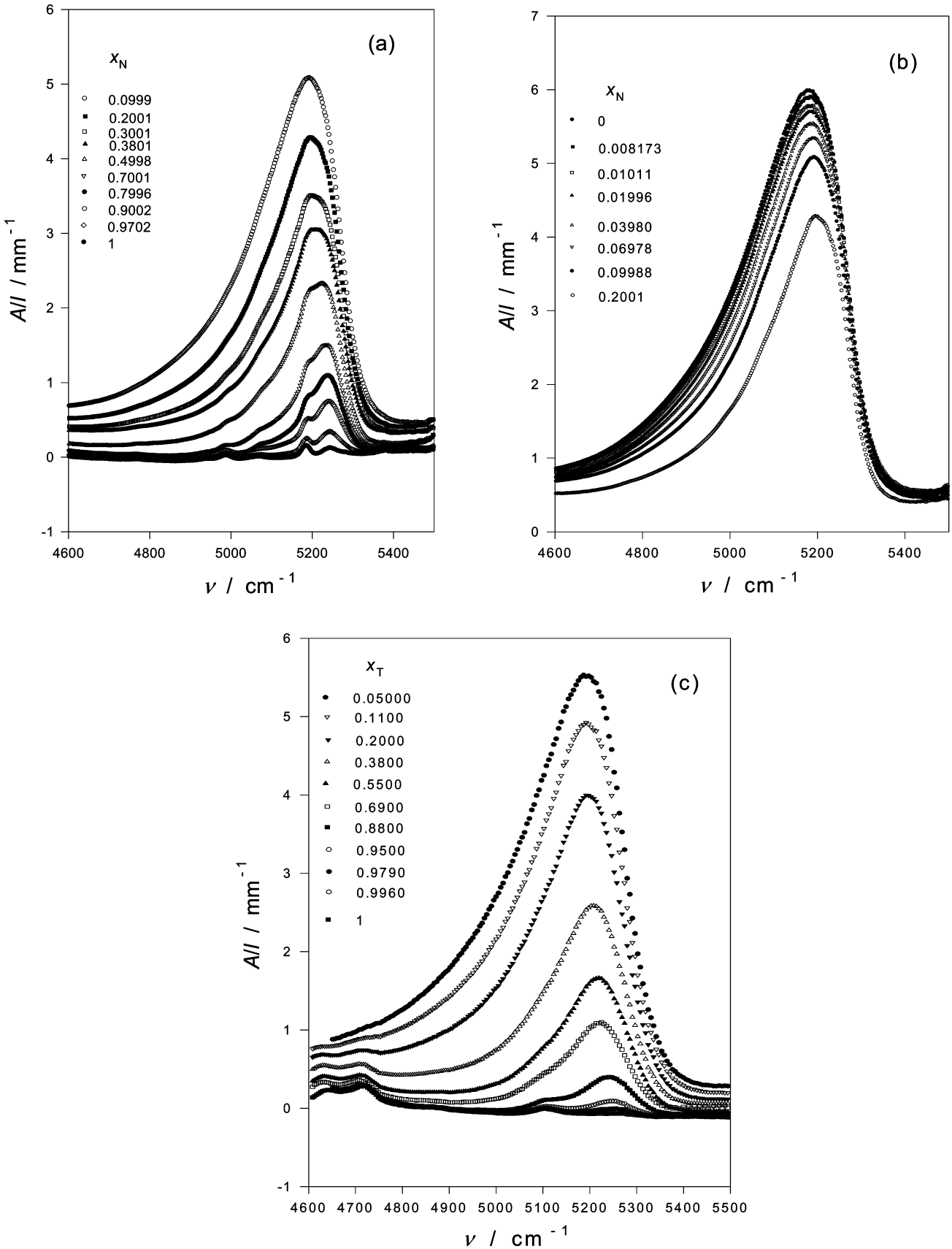

Figure 1. (a) Absorbance divided by the path length, A/l, for acetonitrile (ACN)−H_2O at room temperature. x_N is the mole fraction of ACN. (b) The same as Figure 1(a). (c) The same as Figure 1(a) and 1(b) but for acetone (ACT)−H_2O. x_T is the mole fraction of ACT.

cm^{-1} for the negative bands and ± 15 cm^{-1} for the positive ones sporadically back and forth. We judge these sporadic variations to be due to the systematic error associated with the present single beam measurement. We thus take the average ε^E value in the range 5020 $\pm$ 20 and 5230 $\pm$ 15 cm^{-1} as the representative value of ε^E at each band and plotted it against

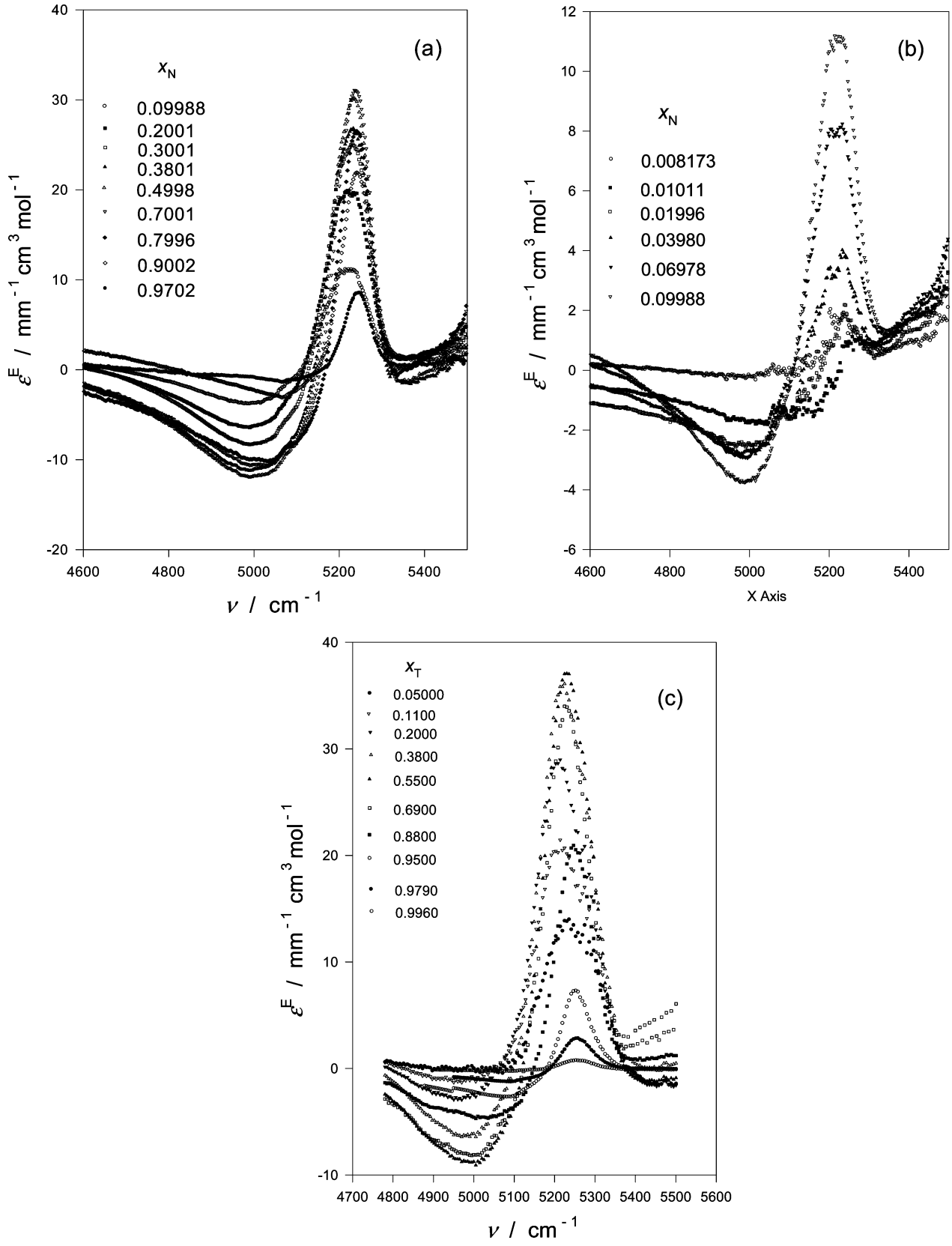

Figure 2. (a) Excess molar absorptivity, ε^E, for acetonitrile (ACN)−H_2O at room temperature. x_N is the mole fraction of ACN. (b) The same as Figure 2(a). (c) The same but for acetone (ACT)−H_2O at room temperature. x_T is the mole fraction of ACT. To convert the units of ε^E to the usual (cm^{-1} dm^3 mol^{-1}), multiply the ordinate by (1/100).

the mole fraction, x_N or x_T, in Figure 3. We stress that ε^E vs x_N (or x_T) curves are shown only at two wavenumbers. There are in fact a series of curves at any given wavenumber, all fixed at zero at x_N (or x_T) = 0 and 1. What are shown in the figure are the maximum (at 5230 cm^{-1}) and the minimum (at 5020 cm^{-1}) curves enveloping other wavenumber series. However, we limit ourselves here to the two, the maximum and the minimum. Also shown in Figure 3 are the random error bars that were calculated

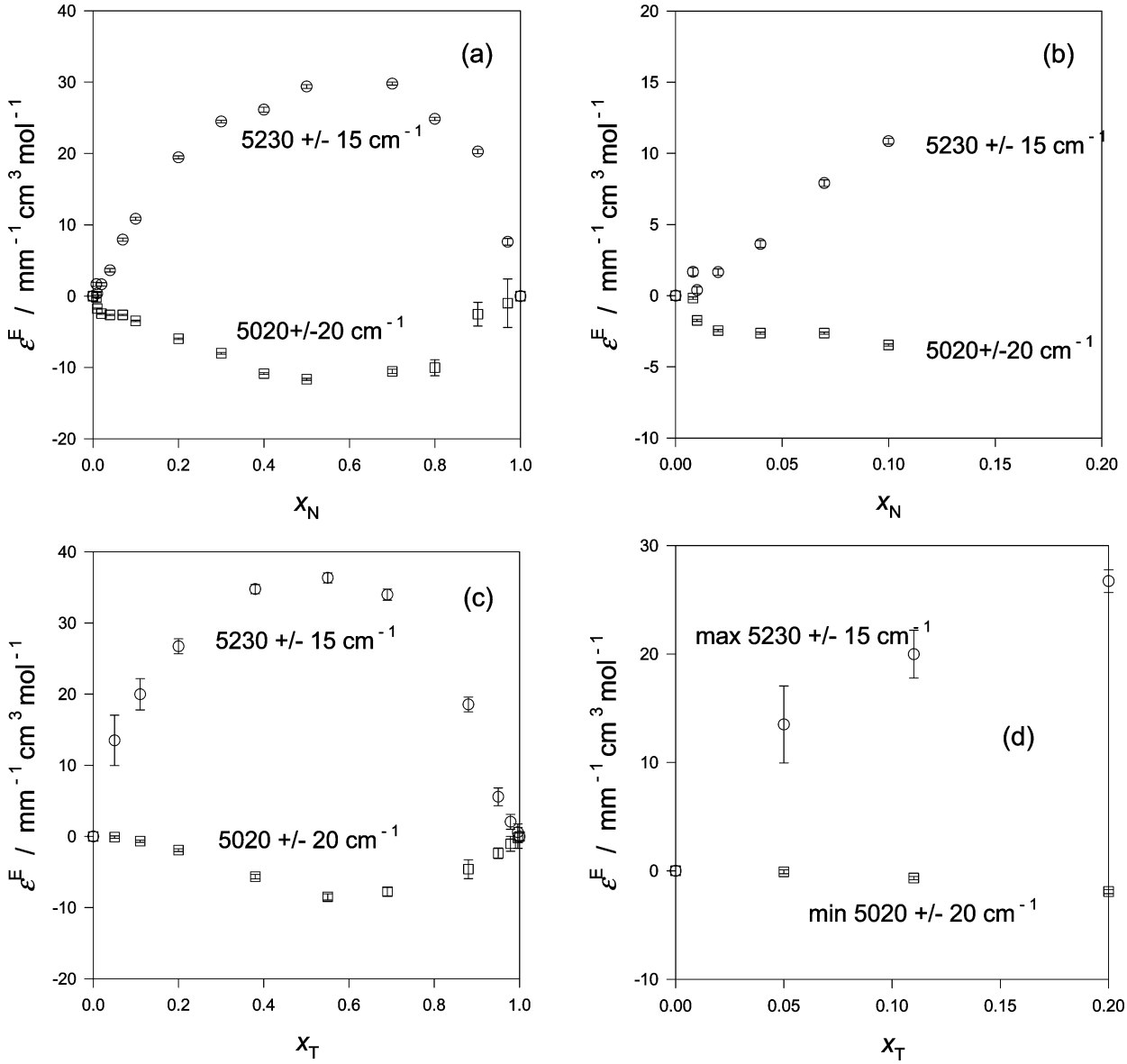

Figure 3. (a) Excess molar absorptivity, ε^E, of the negative band at 5020 ± 20 cm^{-1} and of the positive band at 5320 ± 15 cm^{-1} for acetonitrile (ACN)−H_2O at room temperature. See text for error bars. (b) The same as Figure 3(a) and (b). Figures 3(c) and (d) are the same as Figure 3(a) but for acetone (ACT)−H_2O. To convert the units of ε^E to the usual (cm^{-1} dm^3 mol^{-1}), multiply the ordinate by (1/100).

using the uncertainties in the transmission, t, and that in mole fraction. Those for the path length, l, and the molar volume, V_m, are ignored. Of course, possible systematic errors due to uncertainties in baseline may still exist. Unfortunately, they are not explicitly known. Nevertheless, comparison between ACN−H_2O (Figure 3(a) and (b)) and ACT−H_2O (Figure 3(c) and (d)) reveals a clear difference in the mole fraction dependence of ε^E, particularly for the negative band at about 5020 cm^{-1} in the H_2O-rich region. Namely, for ACN−H_2O, ε^E for the negative band representing the ice-likeness decreases sharply at $x_N = 0.008-0.01$, while that for ACT−H_2O remains almost constant for $x_T < 0.1$. These observations are consistent with the mixing scheme elucidated by our earlier thermodynamics studies on ACN−H_2O and ACT−H_2O discussed in the Introduction. While ACN enhances the hydrogen bond network in its immediate vicinity, the dominant effect on H_2O is that the hydrogen bond probability of bulk H_2O away from solute is progressively reduced up to the threshold $x_N = 0.0094$. This evidently appears as a sharp decrease in the ice-likeness of H_2O. ACT, on the other hand, forms a hydrogen bond directly to the existing network of H_2O and retrains the hydrogen bond connectivity up to $x_T = 0.08$.

To see the x_N and x_T variations of the respective ε^E more clearly, we calculate the excess partial molar absorptivity of ACN, ε_N^E, and that of ACT, ε_T^E, by eq 7. We drew a smooth curve through the data points in Figure 3 by aid of a flexible ruler. We then read the ε^E value off the smooth curve, and the quotient $\delta\varepsilon^E/\delta x_N$ (or δx_T) is approximated to the partial derivative on the far right of eq 7. The values of δx_N (or δx_T) were chosen as $\delta x_N = 0.02$ in the range $x_N < 0.12$, otherwise $\delta x_N = \delta x_T = 0.04$. Such choices are appropriate for the approximation, as discussed at some length earlier.[23] The results, ε_N^E and ε_T^E, are shown in Figure 4. Also indicated by dotted lines are the values of x_N and x_T at point X and Y, the onset and the end point of the transition from Mixing Schemes I to II, and the boundary between Mixing Schemes II and III suggested by our thermodynamic studies. The ε_N^E and ε_T^E data shown in Figure 4 are of course pending on unknown systematic error due to uncertainty in baseline. Nevertheless, the information apparent in Figure 4 is truly instructive. Figure 4(a) indicates that ε_N^E for

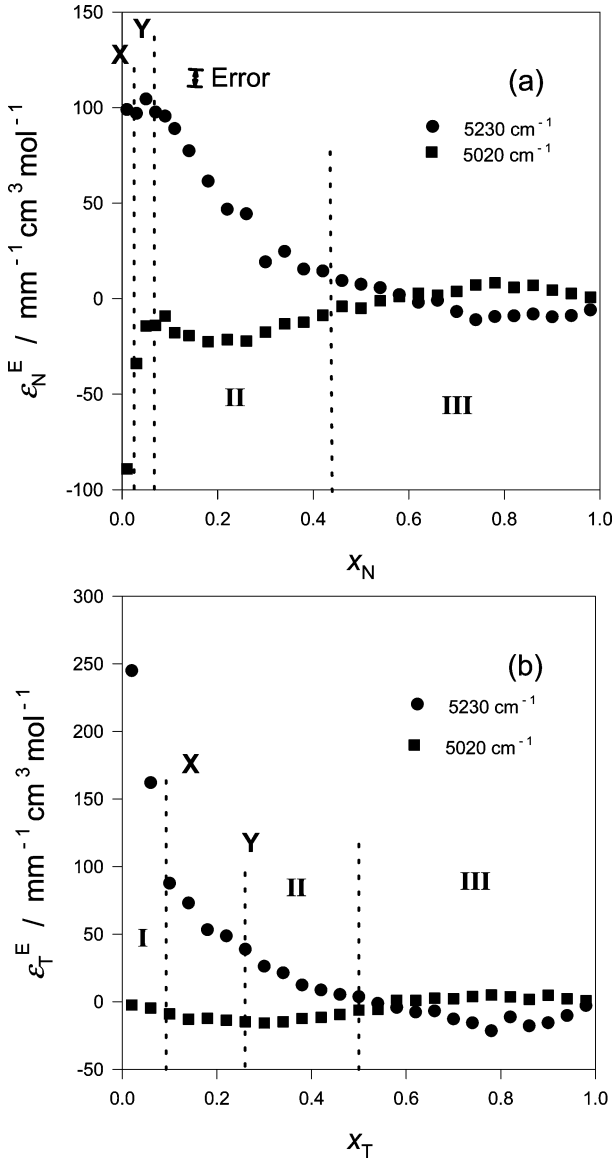

Figure 4. Excess partial molar absorptivity of ACN, ε_N^E, in ACN−H_2O of the negative band 5020 cm^{-1} and the positive band (5230 cm^{-1}) at room temperature. (b) The same but that of ACT, ε_T^E, in ACT−H_2O. To convert the units of ε_N^E (or ε_T^E) to the usual (cm^{-1} dm^3 mol^{-1}), multiply the ordinate by (1/100).

the negative band, the effect of ACN on the ice-likeness, is largely negative at the infinite dilution suggesting the main effect of ACN on bulk H_2O is to reduce ice-likeness. As x_N increases to point X, $x_N = 0.008$, such an effect diminishes rapidly and then remains unchanged to point Y. That for the positive band, on the other hand, seems to stay constant from the infinite dilution up to point Y; i.e., the rate of relative increase of the liquid-likeness due to the effect of ACN stays constant. Thus, the mixing scheme suggested by earlier thermodynamic studies is accompanied by the sharp decrease in the ice-likeness with almost constant effect of the relative increase in the liquid-likeness in the present terminology. For hydrophilic ACT−H_2O, Figure 4(b), the effect of ACT on the negative band (ice-likeness) is nearly zero and remains almost constant, but the effect of increase on the liquid-likeness drops sharply to point X. This is consistent with what a hydrophile does to H_2O. In addition, this suggests that the hydrogen bond connectivity is related to the negative band at 5020 cm^{-1} and the degree of fluctuation to the positive band at 5230 cm^{-1}. For both ACN and ACT−H_2O cases, the x_N (or x_T)-loci of point Y and the boundary between Mixing Schemes II and III are not quite conspicuous as in the thermodynamic studies. However, we note the crossover between the "ice-likeness" and the "liquid-likeness" near but not exactly at the II−III boundary (we thank Reviewer 1 for pointing this out). The latter locus was determined by the intersection of two lines with a shallow angle,[24] and it is not with full confidence. Nonetheless, this observation is instructive since in Mixing Scheme III there is no liquid H_2O present. This point requires a further investigation, however.

Thus, the present many-body analysis on the spectroscopic data adds some more detail into Mixing Scheme I for both aqueous solutions. The effect of a hydrophobe on H_2O manifests itself mainly on the sharp rate of decrease in the negative band (5020 cm^{-1}) characterized qualitatively as the ice-likeness, while that of a hydrophile seems to do to the decrease in the rate of increase of the positive band (5230 cm^{-1}), the liquid-likeness. The descriptive details of Mixing Scheme I and the difference between a hydrophobic and a hydrophilic solute suggested by our earlier thermodynamic studies are now attributed to the difference in its effect on different bands.

It is desirable to learn more about the negative 5020 cm^{-1} and the positive 5230 cm^{-1} bands beyond the qualitative description: the ice-likeness and the liquid-likeness. Indeed, Fornes and Chaussidon[12] deconvoluted the $\nu_2 + \nu_3$ NIR spectrum into three distinctive Gaussian bands, S_0, S_1, and S_2, following the lead by Buijs and Choppin.[25] Here S_0, S_1, and S_2 represent a central H_2O molecule with 0, 1, and 2 protons forming hydrogen bonds with the neighboring H_2O. The ice spectrum was successfully deconvoluted into S_1 and S_2, while that from liquid H_2O was deconvoluted into S_0, S_1, and S_2. (Czarnik-Matusewicz and Pilorz by using the principal component analysis and the two-dimensional correlation analysis suggested that the $\nu_2 + \nu_3$ band consists of three components. However, they also point out that the interpretation about the origin of the three remains debatable.[13]) Thus the nonsymmetry of the $\nu_2 + \nu_3$ band and its variation on temperature rise were attributed to the population changes of these three bands. Then the integral intensities of each deconvoluted band S_0, S_1, and S_2 were used to calculate van't Hoff enthalpy differences between two chosen species. The plots of the logarithm of the ratio of the intensities of a given pair were shown to lie on a straight line against $1/T$. However, the ranges of both temperature and logarithm of the ratio are rather small; the former varies about 0.5×10^{-3} K^{-1} and the latter a fraction of a decade in the natural logarithm. When the ranges of plots for both axes are small, the judgment that the plots lie on a straight line must be made with some caution. More importantly, however, the basic premise of the van't Hoff treatment is that, aside from the debatable issue whether such three distinctive species do indeed exist or not, the absorbance, or its integral, is proportional to the concentration of the species in question. Our starting point of the present analysis is that we accept the possibility of nonlinear relationship between the absorbance and the concentration. Hence we rather avoid following this route. However, the fact that the negative band we call ice-like consists of S_1 and S_2 only and the liquid-like positive band contains a large proportion of S_0 in addition to S_1 and maybe S_2 is instructive.

Finally, we comment on more fundamental issues in learning the nature of the negative and the positive bands. By the strong interaction occurring in aqueous solutions, the vibrational wave functions are altered somewhat. For example, the difference in the wavenumber between the negative and the positive bands

is about 200 cm^{-1}, that corresponds to 2.4 kJ mol^{-1} which is a fraction of a typical hydrogen bond strength. The actual effect on ε^E may be less than this value. If such interactions are operative, then the vibrational wave functions of either the ground or the excited state will be altered not only in the energy gap but also in their degeneracy (or multiplicity). The latter entropic effect alone may introduce skewness in the band. Further theoretical advancement regarding the spectra of excess partial molar absorptibity, ε_B^E, is awaited. In any case, the present approach could be useful in tackling the inevitable many-body problems in aqueous or any other nonideal mixtures.

Acknowledgment. We are thankful for general financial support by the Ministry of Education, Culture, Sports, Science and Technology of Japan. The guest professorship of Y.K. to Chiba University was supported by the Grant-in-Aid for Scientific Research (No. 17073002) from the Ministry of Education, Culture, Sports, Science and Technology of Japan. One of us (K.S.) acknowledges the Sumitomo Foundation Award for Young Researchers and a Collaboration-Research-Foundation Award for Young Researchers from the Graduate School of Science and Technology of Chiba University. The latter two grants helped us to start up the present study.

Supporting Information Available: Table Supp. 1 and Supp. 2 containing the absorbance divided by the optical path length and the excess molar absorptivity data. This material is available free of charge via the Internet at http://pubs.acs.org.

References and Notes

(1) Prigogine, I.; Defay, R. *Chemical Thermodynamics* (trans. by Everett, D. H.); Longman: London, 1954, Chapter XXIV.

(2) Koga, Y. *Solution Thermodynamics and Its Application to Aqueous Solutions: A Differential Approach*; Elsevier: Amsterdam, 2007.

(3) Koga, Y. *J. Phys. Chem.* **1996**, *100*, 5172.

(4) Koga, Y. Netsusokutei. *J. Jpn. Soc. Calorim. Therm. Anal.* **2003**, *30*, 54. Available in a pdf form on request to the author at koga@chem.ubc.ca.

(5) Ref 2, but Chapters III and V.

(6) Ref 2, but Chapter VI.

(7) Nikolova, P.; Duff, S. J. B.; Westh, P.; Haynes, C. A.; Kasahara, Y.; Nishikawa, K.; Koga, Y. *Can. J. Chem.* **2000**, *78*, 1553.

(8) Chen, D. H. C.; Chu, P. M.; Tanaka, S. H.; To, E. C. H.; Koga, Y. *Fluid Phase Equilib.* **2000**, *175*, 35.

(9) Idrissi, A.; Longelin, S.; Sokolic, F. *J. Phys. Chem. B* **2001**, *105*, 6004.

(10) Kister, A. K.; Walman, D. C. *J. Chem. Phys.* **1958**, *62*, 245.

(11) Nicholson, D. E. *J. Chem. Eng. Data* **1960**, *5*, 35.

(12) Fornes, V.; Chaussidon, J. *J. Chem. Phys.* **1978**, *68*, 4667.

(13) Czarnik-Matusewicz, B.; Pilorz, S. *Vib. Spectrosc.* **2006**, *40*, 235.

(14) Saitow, K.; Kobayashi, K.; Nishikawa, K. *J. Solution Chem.* **2004**, *33*, 689.

(15) Li, Q.; Wang, N.; Zhoyu, Q.; Sun, S.; Yu, Z. *Appl. Spectrosc.* **2008**, *62*, 166.

(16) Handa, Y. P.; Benson, G. C. *J. Solution Chem.* **1981**, *10*, 291.

(17) Boje, L.; Hvidt, Aa. *J. Chem. Thermodyn.* **1971**, *3*, 663.

(18) Lide, D. R., Ed., *CRC Handbook of Chemistry and Physics*, 77th ed.; CRC press: Boca Raton, 1996.

(19) Roentgen, W. C. *Ann. Phys.* **1892**, *45*, 91.

(20) Vedamuthu, M.; Singh, S.; Robin, G. W. *J. Phys. Chem.* **1995**, *99*, 9263.

(21) Jetter, K.; Depczyuski, U.; Molt, K.; Niemoeller, A. *Anal. Chim. Acta* **2000**, *420*, 169.

(22) Berry, R. J.; Ozaki, Y. *Appl. Spectrosc.* **2002**, *56*, 1462.

(23) Parsons, M. T.; Westh, P.; Davies, J. V.; Trandum, Ch.; To, E. C. H.; Chiang, W. M.; Yee, E. G. M.; Koga, Y. *J. Solution Chem.* **2001**, *30*, 1007.

(24) Ref 2 but Section [V-5].

(25) Buijs, K.; Choppin, R. G. *J. Chem. Phys.* **1963**, *39*, 2035.

JP901934C